ChemRxiv™

doi.org/10.26434/chemrxiv.7447481.v1

Ferroelectricity and Large Piezoelectric Response of AlN/ScN Superlattice

Mohammad Noor-A-Alam, Oskar Olszewski, Michael Nolan

Submitted date: 11/12/2018 • Posted date: 11/12/2018

Licence: CC BY-NC-ND 4.0

Citation information: Noor-A-Alam, Mohammad; Olszewski, Oskar; Nolan, Michael (2018): Ferroelectricity and Large Piezoelectric Response of AlN/ScN Superlattice. ChemRxiv. Preprint.

Based on density functional theory, we investigate the ferroelectric and piezoelectric properties of the AlN/ScN superlattice. We find that the polar wurzite (w-ScAlN) structure is mechanically and dynamically stable, and is more stable than the nonpolar hexagonal flat configuration. We show that ferroelectric polarization switching can be possible for epitaxially tensile strained superlattice. Due to the elastic constant C33 softening along with an increase in e33, the piezoelectric coefficient d33 of the superlattice is doubled compared to pure w-AlN. The combined enhancement of Born effective charges (Z33) and the sensitivity of the atomic co-ordinates to external strain (\frac{\partial u_{3}}{\partial\eta_{3}}) is the origin of large piezoelectric constant e33. Moreover, we show that epitaxial biaxial tensile strain significantly enhances the piezo-response, so that d33 is seven times larger than that of w-AlN at 4% strain. The tensile strain results in a huge enhancement in e33by increasing Z33 and \frac{\partial u_{3}}{\partial\eta_{3}}, which boosts the piezoelectric coefficient. As both superlattice growth and epitaxial strain are already experimentally demonstrated in wurzite nitrides, our results show a new, more controlled approach to significantly enhance and tune the piezoelectric response of w-AlN materials.

File list (2)

ScAlN-Suplementry.pdf (431.25 KiB) view on ChemRxiv • download file

ScAlN -manuscript-27-11-2018.pdf (526.19 KiB) view on ChemRxiv • download file

Ferroelectrcity and Large Piezoelectric Response of AlN/ScN superlattice

Mohammad Noor-A-Alam, Oskar Z. Olszewski and Michael Nolan
Tyndall National Institute, Lee Maltings, Dyke Parade,
University College Cork, Cork, T12 R5CP, Ireland

I. COMPUTATIONAL DETAILS

Our first-principles calculations are performed in the framework of spin-polarized density functional theory using projector augmented wave (PAW) potentials to describe the core electrons and the generalized gradient approximation (GGA) of Perdew, Burke, and Ernzernhof (PBE) for exchange and correlation as implemented in the Vienna Ab initio Simulation Package (VASP) Perdew *et al.* [1], Kresse and Furthmüller [2], Kresse and Joubert [3] based on a plane-wave basis set. A cutoff energy of 500 eV for the plane-wave expansion is used in all calculations and all structures are fully relaxed until the Hellmann-Feynman forces on all the atoms are less than 10^{-3} eV/Å. The lattice parameters and internal coordinates of the structures are fully relaxed to achieve the lowest energy configuration using conjugate gradient algorithm. Geometry optimization of ScAlN is carried out employing the conjugated gradient technique and the convergence for the total energy is set as 10^{-7} eV. The Brillouin zone is sampled with a Γ -centered k -point mesh of $15 \times 15 \times 15$ for geometry optimizations, while a denser grid of $25 \times 25 \times 25$ is used for electric polarization calculations. Density functional perturbation theory (DFPT) is used to calculate elastic (C_{ij}) and piezoelectric (e_{ij}) tensors. THe modern theory of polarization based upon the Berry phase is employed in the calculation of the electric polarization. The nudged elastic band method (NEB)Henkelman *et al.* [4] with five images is employed to calculate the polarization switching energy barrier. Recently developed solid-state NEB (SSNEB)Sheppard *et al.* [5] has also been used to calculate the barrier as this method allows for relaxation of atomic and cell degrees of freedom.

II. PARTIAL DENSITY OF STATES (PDOS)

[1] J. P. Perdew, K. Burke, and M. Ernzerhof, Phys. Rev. Lett. **77**, 3865 (1996).
[2] G. Kresse and J. Furthmüller, Phys. Rev. B **54**, 11169 (1996).
[3] G. Kresse and D. Joubert, Phys. Rev. B **59**, 1758 (1999).
[4] G. Henkelman, B. P. Uberuaga, and H. Jónsson, The Journal of Chemical Physics **113**, 9901 (2000).
[5] D. Sheppard, P. Xiao, W. Chemelewski, D. D. Johnson, and G. Henkelman, The Journal of Chemical Physics **136**, 074103 (2012).

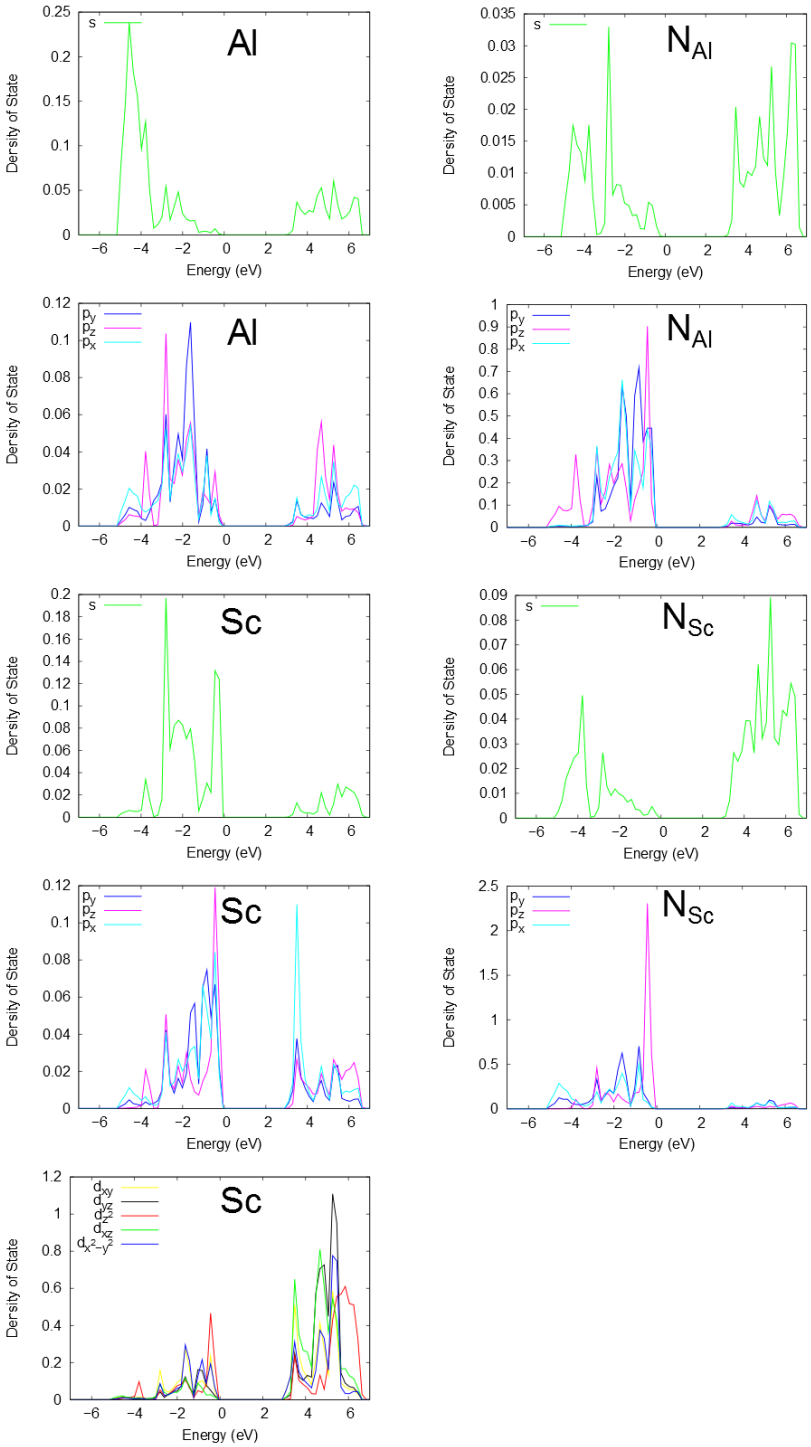


Figure S1. Angular momentum decomposed partial densities of states (PDOS) of Al, N and Sc in w-ScAlN. N_{Al} (N_{Sc}) represents the N on top of Al (Sc).

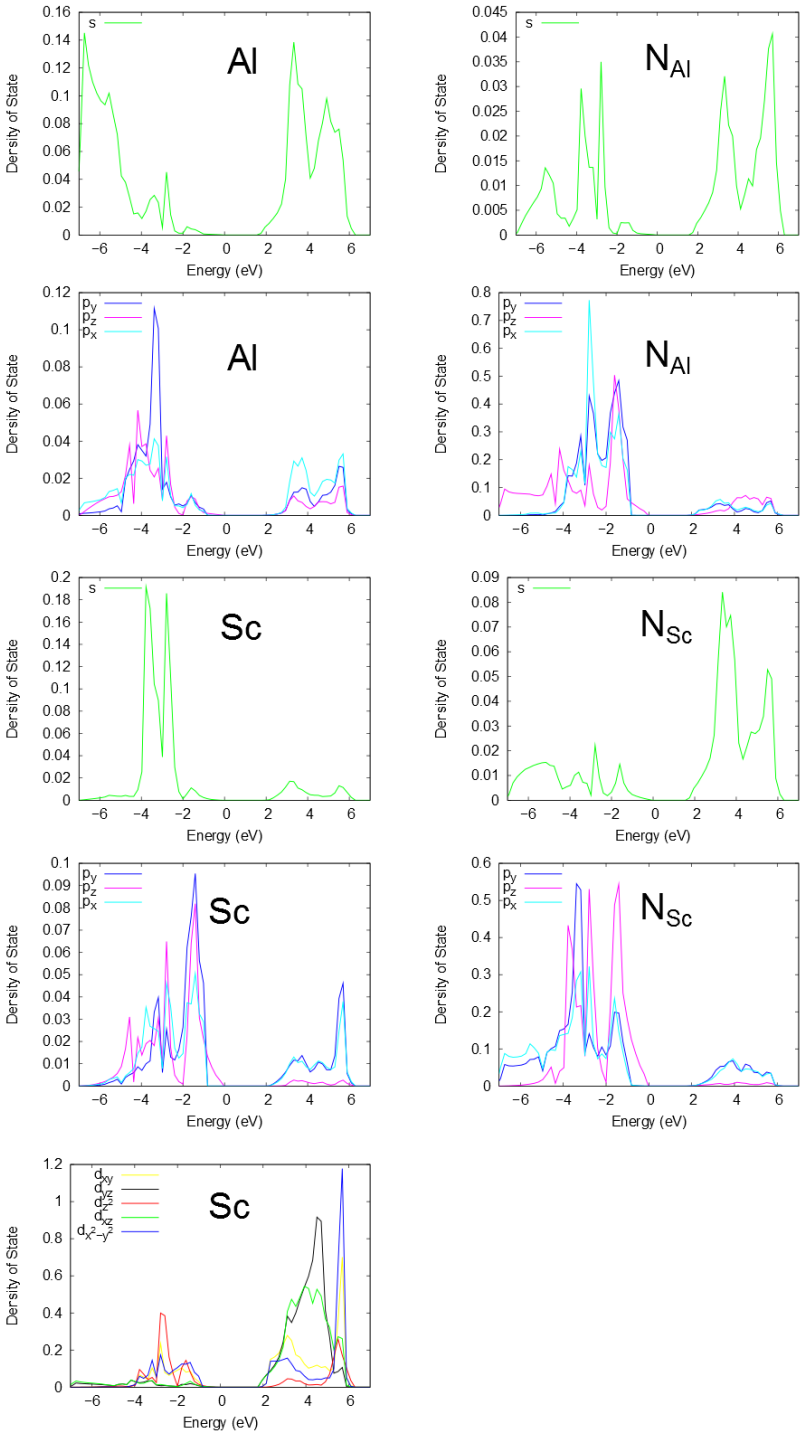


Figure S2. Angular momentum decomposed PDOS of Al, N and Sc in h-ScAlN. N_{Al} (N_{Sc}) represents the N on top of Al (Sc).

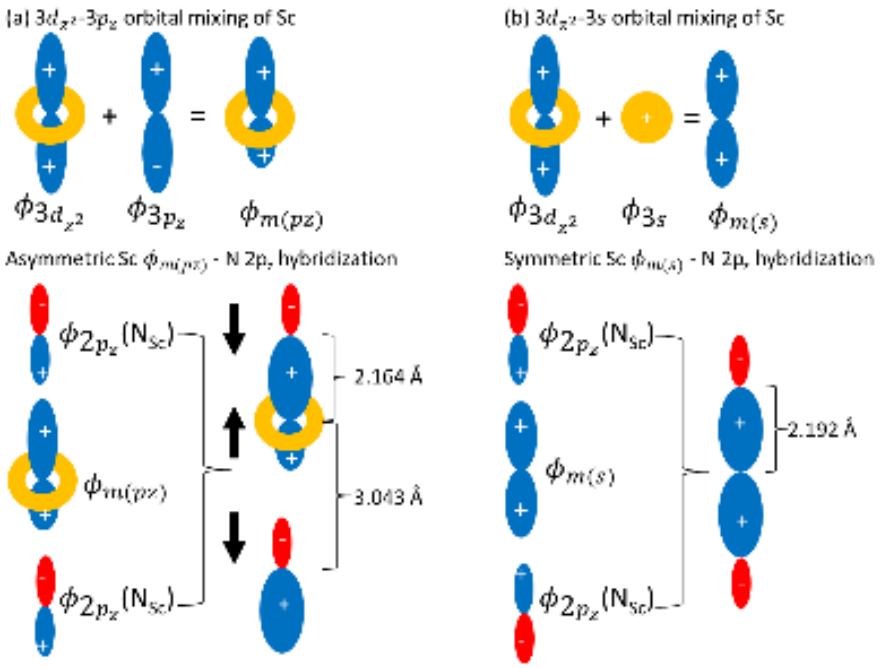


Figure S3. (a) Schematic diagram of asymmetric Sc $\phi_{m(p_z)}$-N $2p_z$ hybridization in w-ScAlN and (b) schematic diagram of symmetric Sc $\phi_{m(s)}$-N $2p_z$ hybridization in h-ScAlN.

ScAlN-Suplementry.pdf (431.25 KiB) view on ChemRxiv • download file

Ferroelectrcity and Large Piezoelectric Response of AlN/ScN superlattice

Mohammad Noor-A-Alam, Oskar Z. Olszewski and Michael Nolan
Tyndall National Institute, Lee Maltings, Dyke Parade,
University College Cork, Cork, T12 R5CP, Ireland

Based on density functional theory, we investigate the ferroelectric and piezoelectric properties of the AlN/ScN superlattice. We find that the polar wurzite (w-ScAlN) structure is mechanically and dynamically stable, and is more stable than the nonpolar hexagonal flat configuration. We show that ferroelectric polarization switching can be possible for epitaxially tensile strained superlattice. Due to the elastic constant C_{33} softening along with an increase in e_{33}, the piezoelectric coefficient d_{33} of the superlattice is doubled compared to pure w-AlN. The combined enhancement of Born effective charges (Z_{33}) and the sensitivity of the atomic co-ordinates to external strain ($\frac{\partial u_3}{\partial \eta_3}$) is the origin of large piezoelectric constant e_{33}. Moreover, we show that epitaxial biaxial tensile strain significantly enhances the piezo-response, so that d_{33} is seven times larger than that of w-AlN at 4% strain. The tensile strain results in a huge enhancement in $e_{33}$by increasing Z_{33} and $\frac{\partial u_3}{\partial \eta_3}$, which boosts the piezoelectric coefficient. As both superlattice growth and epitaxial strain are already experimentally demonstrated in wurzite nitrides, our results show a new, more controlled approach to significantly enhance and tune the piezoelectric response of w-AlN materials.

Over the past two decades, piezoelectric microelectromechanical systems (MEMS) have become attractive in multiple applications, including high frequency and temperature-stable resonators that have significantly miniaturised cell phones, piezoelectric sensors and energy harvesting devices. Suitable non-toxic (lead-free) and cheap piezoelectrics with a high piezoelectric response are required for these devices. In this respect, environment friendly lead-free wurtzite AlN (w-AlN) has already demonstrated significant potential for realizing more complex sensing and mobile communication systems mainly due to the compatibility of AlN devices with complementary metal oxide semiconductor (CMOS). A high Curie temperature, low acoustic and dielectric losses, high acoustic wave velocity, and compatibility with established silicon manufacturing process make AlN a perfect candidate for various MEMS/NEMS devices[1]. High performance RF filters made of AlN based resonators also show great promise for mobile communication systems. However, the low electro-mechanical coupling coefficient, which is closely related to the piezoelectric coefficients, is the main disadvantage of pure w-AlN. Therefore, enhancement of this coupling in AlN based materials in a reliable and tunable way as well as atomistic understanding of the mechanism behind it are the key challenges for both academia and industry[1].

Promisingly, recent experiments have demonstrated a significant enhancement for piezo-response in doped w-AlN[2–4]. For example, a $Sc_{0.5}Al_{0.5}N$ alloy shows a huge (about 400%) increase of the piezoelectric constant d_{33} when compared to pure w-AlN[5]. As the Sc concentration increases, the piezoelectric constant e_{33} increases because of a large increase in the sensitivity of the internal coordinates of the atoms to strain[5, 6]. Such a significant increase in e_{33} along with profound softening of the elastic constant C_{33} arises because of the energy landscape flattening as a result of a competition between the hexagonal and the parent wurtzite phases and drives a tremendous increase in d_{33}[5]. However, the major difficulties with these alloys that prevent their widespread use are (i) the high Sc-doping concentration leads to a phase transition that completely suppresses the piezoelectricity, although the significant enhancement in piezoelectricity is only observed at high Sc concentrations, which are near the phase transition[2] and (ii) the material properties largely depend on the configurations of the dopants[7], which are formed essentially randomly during the sputtering process. It is therefore hard to control the reliability and reproducibility required for device performance. In this regard, an ordered structure such as a superlattice with enhanced piezo-response is explored in this Letter as an alternative approach to realize the fabrication of stable ScAlN alloys with a high concentration of Sc.

Over the last few decades, the superlattices of short-period group-III nitrides have been studied for their optical properties[8–16]. The fabrication of 1:1 wurtzite group-III nitrides with long range ordering by metalorganic vapor phase epitaxy (MOVPE) has demonstrated a new way to design nitrides with desired properties[9]. Piezoelectric properties of such 1:1 superlattices have also been studied theoretically[17], although there is at present no experimental information. Moreover, the atomistic mechanisms behind the piezoelectric enhancement and dynamical or mechanical stability of the structure are not yet clearly understood. In addition, a controlled way to enhance and tune the piezoelectric properties is desired for practical device applications. To our best knowledge, possibility of ferroelectricity in such superlattices has also remained unexplored.

In this Letter, we investigate the origin of the enhanced piezoelectric constants in a 1:1 ScN-AlN superlattice. We show that although wurtzite nitrides are polar materials with large polarization switching barriers that hinder applications in ferroelectric devices,ferroelectric polarization switching can be realized in the superlatrice, which adds new functionalities to wurtzite-structured nitrides. Ferroelectricity in highly Sc doped w-AlN was recently predicted[16], although the phase stability prob-

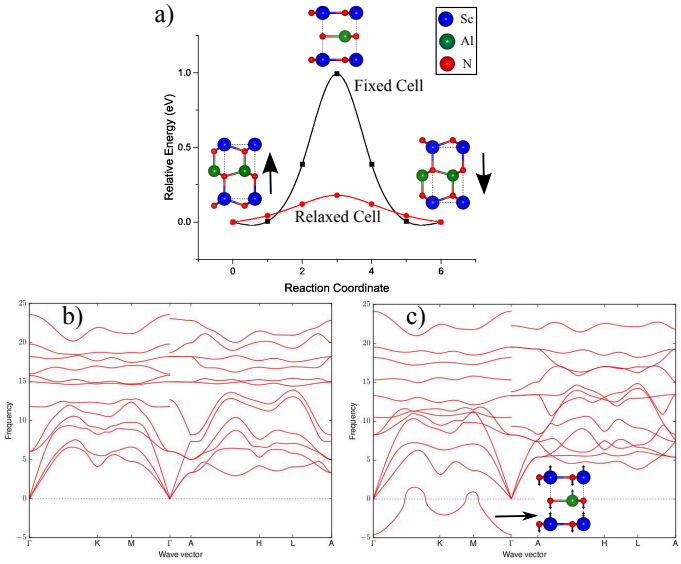


Figure 1. (a) Energy barrier for polarization switching by flatting of Al-N plane. Black curve shows the energy barrier when the unit cell is fixed to polar configuration during the switching, while red curve shows the energy barrier when the unit cell is relaxed using SS-NEB method. (b) and (c) Phonon band structure of w-ScAlN and h-ScAlN, respectively. Inset in (c) shows the atomic displacement of the imaginary mode.

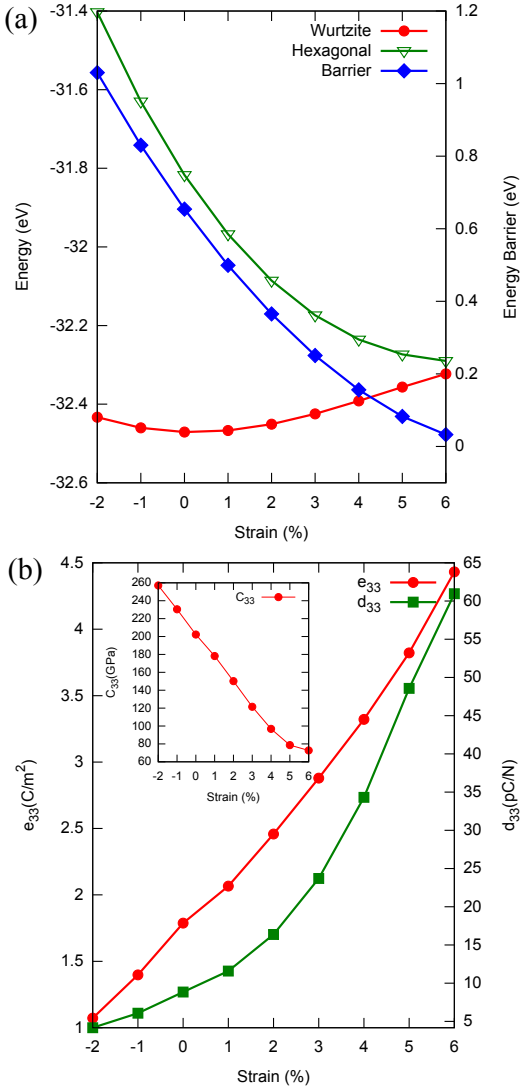


Figure 2. (a) Total energy per formula unit of w-ScAlN and h-ScAlN with epitaxial strain. The energy barrier is defined as the energy difference between the wurtzite and hexagonal phase of ScAlN superlattice, where h-ScAlN has the wurtzite's in-plane lattice parameter. (b) Change in piezoelectric constants (e_{33} and d_{33}) with epitaxial strain. Inset shows the change in elastic constant C_{33} with epitaxial strain.

lem at high Sc concentration still persists[2]. Furthermore, we propose that epitaxial biaxal tensile strain in ScAlN can reduce the polarization switching barrier, and increase d_{33} by a factor of seven compared to pure w-AlN. The applied strain leads the structure closer to a phase transition from wurtzite-like to graphitic structure. A similar enhancement in piezoelectric properties is well-known for ferroelectric perovskites near to the phase-transition region[18]. We also mentioned that epitaxial strain has been intensively studied both theoretically and experimentally for inducing ferroelectricity in paraelectric perovskites[19, 20] and rock-salt non-ferroelectric materials[21].

The ordered wurzite-like ScAlN 1:1 superlattice, shown in Fig 1, consists of one layer of buckled ScN and buckled AlN alternating along the c direction. The calculated lattice constant (a=b) for the w-ScAlN superlatice is 3.33 Å, which is larger than that of pure w-AlN (3.13 Å). The c/a ratio of the superlattice is 1.56, which is slightly lower than that of pure w-AlN (1.60). Two different internal parameters u, a dimensionless parameter that determines the position of the atoms in the unit cell, are calculated (u_{Sc} = 0.416 for Sc and u_{Al}= 0.363 for Al). The u parameter of pure w-AlN (u = 0.382) is in between the these values. The w-ScAlN structure is 0.16 eV lower in energy with respect to the hexagonal (h-ScAlN) structure with u = 0.50, where each flat ScN and flat AlN layer repeats along c direction. The negative formation energy of w-ScAlN (-1.44 eV/atom, which is close to the formation energy of w-GaN[22]) indicates its stability with respect to bulk Al (space group: Fm3m), bulk Sc (space group: P63/mmc) and N_2 molecule. As the w-ScAlN superlattice is a new structure, its mechanical and elastic stability are tested according to the criteria for a hexagonal crystal structure[23]: $C_{11} > C_{12}$, $2C_{13}^2 < C_{33}(C_{11}+C_{12})$, $C_{44} > 0$, $C_{66} > 0$. Considering the five independent elastic constants that we obtain, namely C_{11}= 264.72 GPa, C_{12}= 115.02 GPa, C_{13}= 122.82 GPa, C_{33}= 202.21 GPa, and C_{44}= 67.47 GPa, C_{66}= (C_{11}-C_{12})/2, it can be concluded that the ScAlN superlattice is mechanically stable.

To confirm the dynamical stability of w-ScAlN, the phonon dispersion is also calculated. The absnce of any imaginary modes in the phonon bandstructure con-

firms that the structure is stable or at least structurally metastable. On the other hand, the hexagonal phase shows an imaginary optical phonon mode that has the lowest frequency (i4.58 THz) at the gamma point (Γ) of the Brillouin zone. This soft mode represents a set of atomic displacement where Al or Sc and N atoms are moving opposite direction along c-axis. The lowest imaginary phonon mode at Γ guarantees an identical atomic displacement pattern in each unit cell, which results in a ferroelectric polarization.

w-AlN is a polar material with a spontaneous electric polarization of 0.09 C/m^2 directing from the N layer to the Al layer along the c direction. The spontaneous polarization is calculated using Berry phase technique[24, 25], and the non-polar hexagonal configuration is considered to be paraelectric. However, as the energy difference between wurzite and hexagonal phases for AlN is rather high (*ca.* 0.56 eV/unit cell), ferroelectric switching of this spontaneous polarization is not practical. Additionally, a large structural change during switching and the accompanying wurtzite to hexagonal transition, in which the axial lattice parameters (a and b) lengthen by 6.7% and the c dimensions decreases by 17.94% , hinders switching in bulk w-AlN. We find a significant increase in the spontaneous polarization to 0.24 C/m^2 for ScAlN, which is comparable to perovskite $BaTiO_3$(*ca.* 0.27 C/m^2)[26]. Further strengthening the possibility of ferroelctricity, the polarization switching barrier (0.16 eV/unit cell) of the w-ScAlN superlattice is significantly lower than that of w-AlN. The underlying mechanism for the decrease in this energy difference is due to the fact that there exists a metastable hexagonal ScN phase, although the ground state crystal structure of ScN is rocksalt cubic, and its wurtzite phase is unstable[27, 28]. In fact, the internal parameter u_{Sc} = 0.416 in ScAlN is closer to the value of 0.5 for the hexagonal phase than the wurtzite phase. Note that similar value of u_{Sc} is also observed for the Sc atoms in Sc doped w-AlN[16], where the high concentration of Sc drives the wurzite to hexagonal phase transition by increasing u_{Sc} monotonically.

To understand the origin of ferroelectricity, we compare the Born effective Charge (BEC) of the paraelectric (hexagonal) phase of AlN and the ScAlN superlattice. Our calculated Z^*_{33} for Al in h-AlN is 3.12 |e|, but is 3.35 |e| in h-ScAlN; Z^*_{33} of Nis -3.12 |e| in h-AlN , and for N bound to Al (N bound to Sc) in h-ScAlN Z^*_{33} is -3.36 |e| (-3.81 |e|); Z^*_{33} (Sc) is +3.82 |e|. Clearly, Z^*_{33} values in the paraelectric superlattice are notably larger than both the formal charges and the BECs in paraelectric h-AlN. Larger Z^*_{33} values compared to the formal charges indicate that the atomic displacements associated with the ferroelectric phase transition should be stemming from chemical activities, for example, charge transfer, intra-atomic redistribution of charge density, or rehybridization of covalent bonds. Indeed, a partial density of states (PDOS) analysis (supplementary information Fig. S1 and Fig. S2) indicates that the phase transition from hexagonal to wurtzite is associated with a $3d_{z^2} - 3p_z$ hybridization at the Fermi level, in the Sc atom (Fig. S1). This produces an asymmetric mixed orbital $\phi_{m(p_z)}$ along the z-direction, and causes an asymmetric Sc $\phi_{m(p_z)}$-N $2p_z$ hybridization (at the Fermi level) that results in an off-center displacement along the z-direction. $3d_{z^2} - 3s$ orbital mixing is present in h-ScAlN, in the energy range of -4eV to -2eV (Fig. S2). However, this mixing produces a symmetric orbital $\phi_{m(s)}$, and therefore symmetric Sc$\phi_{m(s)}$-N $2p_z$ hybridization does not result in an off-center displacement. On the other hand, the Al-N layer undergoes sp^2-type to sp^3-type hybridization during the phase transition from hexagonal to wurtzite. Note that 'd^0-ness' with hybridization also plays vital role in driving the ferroelectric transition in $YMnO_3$[29–33].

Table I. Born Effective Charges (Z^*_{33}) (|e|), $\frac{\partial u_3}{\partial \eta_3}$, $e^{int}_{33}(k)$ (C/m^2) , e^{int}_{33} (C/m^2), e^{clamp}_{33}(C/m^2) and total e_{33}(C/m^2).

Structure	Atom	Z^*_{33}	$\frac{\partial u_3}{\partial \eta_3}$	$e^{int}_{33}(k)$	e^{int}_{33}	e^{clamp}_{33}	e_{33}
w-AlN	Al	2.680	0.093	0.470	1.880	-0.423	1.457
	N	-2.678	-0.093	0.470			
w-ScAlN	Al	2.810	0.109	0.508	2.370	-0.586	1.784
	Sc	3.056	0.134	0.683			
	N_{Al}	-3.135	-0.114	0.592			
	N_{Sc}	-2.727	-0.130	0.587			
w-ScAlN (5%)	Al	2.938	0.229	1.013			
	Sc	3.252	0.202	0.992	3.995	-0.181	3.814
	N_{Al}	-3.344	-0.187	0.942			
	N_{Sc}	-2.844	-0.244	1.048			

Indeed, a large structural change is still required for the polarization switching. During the transition from wurtzite to the intermediate hexagonal phase required for ferrroelectric switching, the necessary 6.3% increase in the in-plane lattice parameters and the 15.80% decrease in c-direction are likely to cause the bulk crystal to crack. On the other hand, when the crystal structure is not allowed to change in-plane, the energy difference between the wurtzite and hexagonal phases of the ScAlN superlattice, with wurtzite's in-plane lattice parameters, is about 0.63 eV, which is too high for practical memory devices. To understand the origin of this, the phonon band structure for the paraelectric (hexagonal) phase is computed using the basal plane lattice parameters fixed at those of w-ScAlN and allowing the c parameter to relax. The same imaginary mode is present at the Γ point and this mode becomes even softer (i11.60 THz), indicating that the polar wurtzite structure is energetically preferable with respect to hexagonal phase, and in-plane lattice expansion during switching reduces the energy barrier for polarization switching. Therefore, we suggest that an epitaxially biaxial-tensile-strained thin film forced to have the basal plane lattice parameters matched to the substrate by forming a coherent film-substrate interface, and free to relax only along the c-direction, can be ideal

for realizing ferroelectric switching. Such epitaxial strain can additionally prevent the thin film cracking during polarization switching.

The switching barrier can also be profoundly decreased by epitaxial tensile strain as shown in Fig. 2(a). In our ordered structure, we find that an epitaxial biaxal tensile strain plays a similar role as the concentration of Sc, in that both internal parameters increase monotonically with the tensile strain. Furthermore, the switching barrier can be dramatically reduced; for example, at 5% biaxial strain, the energy barrier is only 0.08 eV/unit cell, which is smaller than that of perovskite $PbTiO_3$(about 0.2 eV/unit cell)[26]. It should be mentioned that epitaxial strain has been experimentally demonstrated as an effective approach to engineer ferroectricity in other non-ferroelectric materials[19–21, 34].

For practical device applications such as resonators, the out of plane piezoelectric constants determine device performance. The piezoelectric response of the w-ScAlN superlattice is calculated to be $e_{33} = 1.78 C/m^2$(Table 1). This is larger than that of pure w-AlN ($1.46 C/m^2$). Although disordered Sc-doped AlN has a much larger piezoelectric constant of 3.1 C/m^2 , that result is achieved for high Sc doping levels (≈50%) which induce the phase transition to the hexagonal structure that completely removes the piezoelectric effect.

To understand the origin of large piezoelectric constant, e_{33} can be decomposed into two parts[35]:

$$e_{33}=e_{33}^{clamp} + \sum_k e_{33}^{int}(k) = e_{33}^{clamp} + \sum_k \frac{2e}{\sqrt{3}a^2} Z_{33}^*(k) \frac{du_3(k)}{d\eta_3}$$

The clamped-ion term (e_{33}^{clamp}) arises from the contributions of electrons when the ions are frozen at their zero-strain equilibrium internal atomic coordinates (u); and the internal-strain (e_{33}^{int}) terms arises from the contribution from internal microscopic atomic displacements in response to a macroscopic strain. In our case, the strain (η_3) is applied in the z-direction. Here, k runs over all the atoms in the unit cell, a is the in-plane lattice constant, and e is the electron charge. The Born effective charge (Z_{33}^*(k)) of k-th atom is calculated by the Berry-phase approach. The response of the k-th atom's internal coordinate along c-direction (u_3 (k)) to a macroscopic strain (η_3) is measured by $\frac{du_3(k)}{d\eta_3}$. From Table 1, it is clear that both BEC and internal-response for each atom in w-ScAlN are larger than in w-AlN. Therefore, e_{33} is enhanced for the w-ScAlN superlattice compared to w-AlN. Note that the value of e_{33}^{int} for w-ScAlN, 2.37 C/m^2, is significantly larger than for w-AlN, 1.88 C/m^2, although the contribution from the electrons in w-ScAlN (-0.59 C/m^2) is only slightly larger than in w-AlN (-0.42 C/m^2). Interestingly, we find that all the atoms contribute almost equally.

If we now consider epitaxial biaxal tensile strain, the BEC and internal response term increase significantly. For example, at 5% strain, the internal-response term for each atom is almost doubled compared to w-ScAlN at zero strain. Additionally, e_{33}^{clamp} decreases with increasing strain, which also increases e_{33}. Therefore, we conclude that the larger e_{33} of the w-ScAlN superlattice under epitaxial strain primarily originates from the large increase in the BEC and the internal-response of atoms, with electronic contribution also playing a role at large strain.

Using e_{33} and C_{33}, we estimate d_{33}as ~ e_{33}/C_{33}[5]. Our calculated d_{33} of w-ScAlN (8.84 pC/N) is double that of w-AlN (4.08 pC/N), because of the significant increase in e_{33} and decrease in C_{33} (358.34 GPa in w-AlN to 202.21 GPa in w-ScAlN). As mentioned above, epitaxial biaxal tensile strain significantly enhances e_{33}, and it also profoundly softens C_{33} (shown in Fig. 2). Consequently, we predict a significant enhancement in d_{33} with applied biaxial strain . For example, at a moderate 4% strain, d_{33} becomes about 35 pC/N, which is significantly larger than the highest d_{33} reported for unstable Sc-doped w-AlN.

Two interesting points should be mentioned. Firstly, only C_{33} is linearly decreasing with strain, as the other elastic coefficients remain essentially unaffected. This suggests a controlled approach to tune both the elastic and piezoelectric properties along only the c-direction while keeping the sample unaffected in-plane, which is of great benefit for device design. Secondly, as a consequence of the first point, the elastic stability criteria [$2C_{13}^2 < C_{33}(C_{11}+C_{12})$][23] no longer holds at 5% or larger strain, although the dynamical stability criterion (no imaginary phonon mode for all wave vectors) is still valid at 5% strain. Therefore, we propose that the ideal epitaxial tensile strain will be in the range of 3-4%.

In conclusion, we show that a 1:1 w-ScAlN superlattice is mechanically stable and posseses a ferroelectric spontaneous electric polarization. The barrier for ferroelectric switching can be significantly tuned with epitaxial tensile strain, indicating the possibility of ultrathin ferroelctric films. More importantly, the superlattice exhibits significantly larger piezoelectric response compared to pure w-AlN. The origin of large piezoelectric constant e_{33} is a combination of an enhancement in Born effective charges (Z_{33}) and the sensitivity of atomic co-ordinates with respect to external strain ($\frac{\partial u_3}{\partial \eta_3}$). In addition, the softening of the C_{33} elastic constant further promotes a larger d_{33}. We demonstrate that epitaxial bi-axial tensile strain can significantly enhance the piezo-response. For example, d_{33} is about seven times larger than pure w-AlN. The applied tensile strain enhances $e_{33}$by increasing Z_{33} and $\frac{\partial u_3}{\partial \eta_3}$, together with a pronounced softening of C_{33}, which then significantly increases the value of d_{33}. As both superlattice growth and epitaxial strain have been previously experimentally demosntrated in wurzite nitrides, these results show a novel approach to add new functionalities such as ferroelectricity and tunable piezoelectrictricity to wurzite nitrides.

ACKNOWLEDGMENTS

This publication has emanated from research conducted with the financial support of Science Foundation Ireland (SFI) and is co-funded under the European Regional Development Fund under Grant Number 13/RC/2077. The calculations were performed using the high-performance computing facilities of the Tyndall National Institute. The authors would also like to acknowledge Analog Devices, Inc., for supporting this research.

[1] M. A. Moram and S. Zhang, J. Mater. Chem. A **2**, 6042 (2014).

[2] M. Akiyama, T. Kamohara, K. Kano, A. Teshigahara, Y. Takeuchi, and N. Kawahara, Advanced Materials **21**, 593 (2009).

[3] M. Uehara, H. Shigemoto, Y. Fujio, T. Nagase, Y. Aida, K. Umeda, and M. Akiyama, Applied Physics Letters **111**, 112901 (2017).

[4] K. R. Talley, S. L. Millican, J. Mangum, S. Siol, C. B. Musgrave, B. Gorman, A. M. Holder, A. Zakutayev, and G. L. Brennecka, Phys. Rev. Materials **2**, 063802 (2018).

[5] F. Tasnádi, B. Alling, C. Höglund, G. Wingqvist, J. Birch, L. Hultman, and I. A. Abrikosov, Phys. Rev. Lett. **104**, 137601 (2010).

[6] C. Tholander, I. A. Abrikosov, L. Hultman, and F. Tasnádi, Phys. Rev. B **87**, 094107 (2013).

[7] H. Momida, A. Teshigahara, and T. Oguchi, AIP Advances **6**, 065006 (2016).

[8] S. Y Woo, M. Bugnet, H. P T Nguyen, S. Zhao, Z. Mi, and G. A. Botton, "Atomic-scale compositional fluctuations in ternary iii-nitride nanowires," in *European Microscopy Congress 2016: Proceedings* (American Cancer Society) pp. 550–551.

[9] P. Ruterana, G. Nouet, W. Van der Stricht, I. Moerman, and L. Considine, Applied Physics Letters **72**, 1742 (1998).

[10] V. Ranjan, S. Bin-Omran, D. Sichuga, R. S. Nichols, L. Bellaiche, and A. Alsaad, Phys. Rev. B **72**, 085315 (2005).

[11] V. Ranjan, S. Bin-Omran, L. Bellaiche, and A. Alsaad, Phys. Rev. B **71**, 195302 (2005).

[12] S. Wei, T. Chee-Keong, and T. Nelson, Scientific Reports **7**, 6671 (2017).

[13] G. Staszczak, I. Gorczyca, E. Grzanka, J. Smalc-Koziorowska, G. Targowski, R. Czernecki, M. Siekacz, S. Grzanka, C. Skierbiszewski, T. Schulz, N. E. Christensen, and T. Suski, physica status solidi (b) **254**, 1600710 (2017).

[14] Z. L. Miao, T. J. Yu, F. J. Xu, J. Song, L. Lu, C. C. Huang, Z. J. Yang, X. Q. Wang, G. Y. Zhang, X. P. Zhang, D. P. Yu, and B. Shen, Journal of Applied Physics **107**, 043515 (2010).

[15] L. Lymperakis, T. Schulz, C. Freysoldt, M. Anikeeva, Z. Chen, X. Zheng, B. Shen, C. Chèze, M. Siekacz, X. Q. Wang, M. Albrecht, and J. Neugebauer, Phys. Rev. Materials **2**, 011601 (2018).

[16] S. Zhang, D. Holec, W. Y. Fu, C. J. Humphreys, and M. A. Moram, Journal of Applied Physics **114**, 133510 (2013).

[17] P. Daoust, P. Desjardins, R. A. Masut, V. Gosselin, and M. Côté, Phys. Rev. Materials **1**, 055402 (2017).

[18] M. Budimir, D. Damjanovic, and N. Setter, Phys. Rev. B **72**, 064107 (2005).

[19] Y. Zhang, J. Wang, M. P. K. Sahoo, T. Shimada, and T. Kitamura, Phys. Chem. Chem. Phys. **19**, 26047 (2017).

[20] Y. Zhang, M. P. K. Sahoo, T. Shimada, T. Kitamura, and J. Wang, Phys. Rev. B **96**, 144110 (2017).

[21] E. Bousquet, N. A. Spaldin, and P. Ghosez, Phys. Rev. Lett. **104**, 037601 (2010).

[22] A. Zoroddu, F. Bernardini, P. Ruggerone, and V. Fiorentini, Phys. Rev. B **64**, 045208 (2001).

[23] F. Mouhat and F.-X. Coudert, Phys. Rev. B **90**, 224104 (2014).

[24] R. D. King-Smith and D. Vanderbilt, Phys. Rev. B **47**, 1651 (1993).

[25] D. Vanderbilt and R. D. King-Smith, Phys. Rev. B **48**, 4442 (1993).

[26] F. Simuck, P. Krishna Chaitanya, N. Serge M., E. Markus, L. Ying Wai, and C. Valentino R., Scientific Reports **7**, 43482 (2017).

[27] N. Farrer and L. Bellaiche, Phys. Rev. B **66**, 201203 (2002).

[28] N. Takeuchi, Phys. Rev. B **65**, 045204 (2002).

[29] M.-A. Oak, J.-H. Lee, and H. M. Jang, Phys. Rev. B **84**, 153106 (2011).

[30] J. Kim, K. C. Cho, Y. M. Koo, K. P. Hong, and N. Shin, Applied Physics Letters **95**, 132901 (2009).

[31] C. Zhong, Q. Jiang, H. Zhang, and X. Jiang, Applied Physics Letters **94**, 224107 (2009).

[32] M.-A. Oak, J.-H. Lee, H. M. Jang, J. S. Goh, H. J. Choi, and J. F. Scott, Phys. Rev. Lett. **106**, 047601 (2011).

[33] S. Song, D. Kim, H. M. Jang, B. C. Yeo, S. S. Han, C. S. Kim, and J. F. Scott, Chemistry of Materials **29**, 7596 (2017).

[34] X.-Z. Lu and J. M. Rondinelli, Nature Materials **15**, 951 (2016).

[35] F. Bernardini, V. Fiorentini, and D. Vanderbilt, Phys. Rev. B **56**, R10024 (1997).

ScAlN -manuscript-27-11-2018.pdf (526.19 KiB) view on ChemRxiv • download file